DOI: 10.35840/2631-5084/5544

VIBGYOR ePress

International Journal of
Nanoparticles and Nanotechnology

In-Vitro Cytotoxicity Assessment and Cellular Uptake Study of Novel FluoDot Nanoparticles on Human Cervical Carcinoma Cells

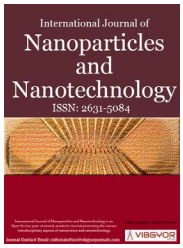

ISSN: 2631-5084

Aseno Sakhrie[1], Jingwen Ding[2], Ankarao Kalluri[2], Cunxia Liu[1,3], Challa V Kumar[2*] and Mazhar I Khan[1*]

[1]*Department of Pathobiology and Veterinary Science, University of Connecticut, 06269, USA*

[2]*Department of Chemistry, University of Connecticut, 06269, USA*

[3]*Institute of Poultry Science, Shandong Academy of Agriculture Sciences, Jinan City, Shandong, China*

Abstract

Protein-based nanoparticles have unique properties, such as low toxicity, biocompatibility, and biodegradability, making them ideal for biological applications. These include vaccine delivery, cancer therapy, and cell imaging. Therefore, here we report the cellular uptake, cell viability and cytotoxicity evaluation of BSA-derived nanoparticles. Cytotoxicity was evaluated in-vitro in HeLa cells using a the MTT (3-(4,5-dimethylthiazol-2-yl)-2,5-diphenyl-2H-tetrazolium bromide) colorimetric assay. The assay revealed dose-dependent decrease in cell viability when the cells were treated with NP concentration ranging from 200 µg/ml - 3.125 µg/ml. These results were confirmed by flow cytometry assay. The estimated IC50 concentration was 26.4 µg/ml. There was a clear uptake by the cells after 30 minutes of incubation; furthermore, an hour later the nanoparticles reached the cytoplasm. The study's results contribute to the understanding of the intracellular uptake, accumulation, and biological impact of the BSA nanoparticles which is important for their successful implementation in medical applications. These findings provide valuable insights into the potential applications of protein-based nanoparticles in vaccine delivery, drug delivery and biomedical imaging.

Keywords

Nanoparticles, Cytotoxicity, Flow cytometry, Cell uptake 4, MTT assay 5

Introduction

During the past few decades, biomedical nanotechnology has been gaining importance for applications in drug delivery [1,2], cell imaging [3], cancer therapy [4] and disease diagnosis [5,6]. Nanoparticles (NP) are tiny particles measured in nanometers and they are often made from polymers, inorganic materials, metals, semiconductors, lipids, carbohydrates, or proteins [7]. Among these, protein-based NPs have distinct advantages over others due to their low toxicity, biocompatibility, and facile biodegradability [8]. Properties such as size, shape, surface properties, and stability of the nanoparticles are crucial for the use of protein NP in cellular toxicity, uptake, distribution, accumulation. These protein-based NPs have a wide range of applications in biology,

***Corresponding author:** *Challa V Kumar, Department of Chemistry, University of Connecticut; Mazhar I Khan, Department of Pathobiology and Veterinary Science, University of Connecticut, 06269, USA*

Accepted: May 18, 2024; **Published:** May 20, 2024

Citation: Sakhrie A, Ding J, Kalluri A, Liu C, Kumar CV, et al., (2024) *In-Vitro* Cytotoxicity Assessment and Cellular Uptake Study of Novel FluoDot Nanoparticles on Human Cervical Carcinoma Cells. Int J Nanoparticles Nanotech 9:044

including cell imaging [9,10], and drug delivery [11-15].

In this study, we chose to examine serum albumin derived nanoparticles, since albumin is present in all mammals, is more biocompatible, and it can be matched with each species or even individuals. Bovine serum albumin has been used extensively to prepare protein nanoparticles and it binds to a variety of ligands such as fatty acids [16], hormones [17], metal ions [18], peptides [19,20], dyes [21], and drugs [22]. Their quick and safe entry into cells is an essential step for NP-based imaging or therapy. Additionally, the intracellular fate of NPs is critical to their success, considering that these carriers are intended to deliver specific molecules (i.e., genes, drugs, and contrast agents) to the cytosol, nucleus, or other specific intracellular sites. Since the NP has been designed for biomedical and pharmaceutical applications, therefore its ability to penetrate or permeate through the biological barriers should be evaluated. Understanding how NPs penetrate cells is crucial because it determines their function, intracellular destiny, and biological impact [23-25].

As part of our analysis, we examined the cellular uptake of nanoparticles and assessed their toxicity using an *in vitro* cytotoxicity assay and flow cytometry, as depicted in Scheme 1. Understanding how nanoparticles are internalized by cells helps optimize their design to enhance cellular uptake and consequently, the delivery of therapeutic payloads. Out of the different cytotoxicity assays available, we used MTT (3-(4,5-dimethylthiazol-2-yl)-2,5-diphenyl-2H-tetrazolium bromide) assay to assess the viability of the cells due to its sensitivity and reliability in indicating cellular metabolic activity. Initially devised by Mosmann, et al. in 1983 [26], this method serves as a quantitative measure of cell viability in culture and functions as a quantitative assay. It is a sensitive assay and measures the growth rate of cells, by virtue of a linear relationship between cell activity and absorbance. The MTT reagent is a mono-

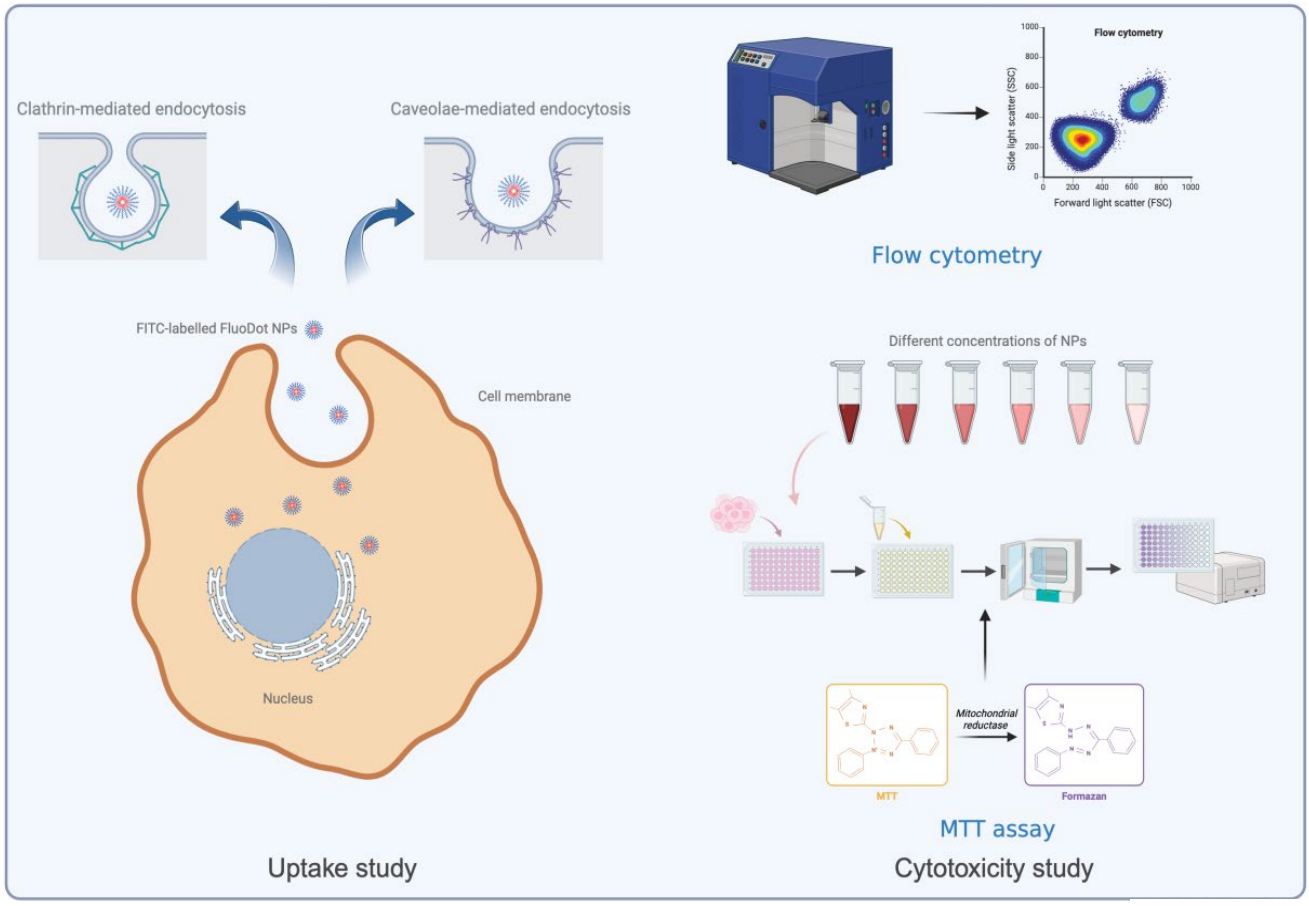

Scheme 1: The entry of nanoparticles (NPs) into cells was observed by employing FluoDot NPs labelled with FITC, while the toxicity at increasing NP concentrations was assessed using the MTT cytotoxicity assay and flow cytometry.

tetrazolium salt comprising of a positively charged quaternary tetrazole ring core containing four nitrogen atoms surrounded by three aromatic rings including two phenyl moieties and one thiazolyl ring which reduces viable cells containing NAD(P)H-dependent oxidoreductase enzymes to formazan [27-29]. This reagent specifically evaluates mitochondrial activity in living cells, as mitochondrial dehydrogenase enzymes cleave the tetrazolium ring resulting in the formation of purple formazan, soluble in dimethyl sulfoxide (DMSO). This compound's fluorescence intensity allows for the quantification of cell proliferation, as it can penetrate both the cell membrane and the mitochondrial inner membrane of viable cells, producing measurable results.

In our investigation, we utilize flow cytometry to evaluate the viability of cell populations. This technique operates on the principle that dead cells display a loss of membrane integrity, distinguishing them from live cells [30]. Various dyes are employed for this purpose, each designed to selectively interact with either live or dead cells. Notably, propidium iodide, a dye commonly utilized in flow cytometry, is specifically adept at detecting dead cells due to its inability to penetrate intact membranes of live cells [31-34]. Its dual positive charge effectively prevents entry into live cells, making it an invaluable tool for discerning cell viability within heterogeneous populations. By leveraging the specificity of propidium iodide and the analytical power of flow cytometry, we aim to precisely characterize the cellular response to nanoparticle exposure and elucidate key insights into their biological effects.

Materials and Methods

Materials

For our study, HeLa cells (Human cervical carcinoma cells) (ATCC, CCL-2) were purchased from ATCC (Manassas, VA, USA). GibcoTM Dulbeco's Modified Eagles Medium (DMEM), Gibco™ Antibiotic-Antimycotic (amphotericin B, penicillin, streptomycin), Gibco™ fetal bovine serum (FBS), Gibco™ phosphate buffered saline and Gibco™ trypsin-EDTA was purchased from Thermo Fisher Scientific (Waltham, MA, USA). TACS MTT Cell Proliferation Assay was purchased from R&D Systems (Minneapolis, MN, USA, 4890-050-K). Invitrogen™ Hoechst 33342, Invitrogen™ CellMask™ plasma membrane stains and Invitrogen™ propidium iodide was purchased from Thermo Fisher Scientific (Waltham, MA, USA). 35 mm glass bottom dish with No 1.5 coverslip was purchased from MatTek Life Sciences (Ashland. MA, USA) and 96-well tissue culture plate was purchased from Falcon BD Bioscience (San Jose, CA, USA).

Synthesis of FluoDot24-FITC

BSA-derived nanoparticles were prepared by following methods as reported in our collaborator's lab [35]. In brief, dodecanedioic acid was activated with EDC and coupled with the amine groups of BSA (50 mM phosphate buffer, pH 8.0), labeled with FITC, and the resulting FluoDot24-FITC particles were purified by dialysis (25 kDa molecular weight cut off) against 50 mM phosphate buffer (pH 8.0). Formation of the nanoparticles was confirmed by dynamic light scattering, and agarose gel electrophoresis, as described in the thesis.

Nanoparticle uptake assay

The protocol outlined by Da silva, et al. was modified and appliedhere [36]. HeLa cells were grown in 35 mm No. 1.5 coverslip bottom dishes from MatTek with clear glass bottom. The cells were incubated at 37 °C for 24 hours. The cells were then treated with FITC labeled FluoDot NPs at 10 ug/ml concentration and incubated at 30 min, 1, 6, 12 and 24 hours. At the end of each incubation period the NPs were rinsed out using PBS and the cells were stained with CellMask™ Deep red Plasma Membrane stain for 10 min at 37 °C. After the incubation, the staining solution was removed and rinsed with PBS three times. This was followed by addition of a sufficient volume of Hoechst 33342 working solution to completely cover the sample. An aluminum foil was placed over the sample to protect it from light and incubated at room temperature for 5-10 minutes. The live cells image was taken immediately using a Nikon A1R Spectral Confocal microscope equipped with a 60X objective lens. Imaging was conducted at an excitation/ emission wavelength of 460/490 nm for FITC and 649/666 nm for the CellMask™ Deep red Plasma Membrane stain.

In vitro cytotoxicity of FluoDot determined using an MTT assay

The *in vitro* cytotoxicity of the FluoDot NPs were determined by using TACS MTT Cell Proliferation Assay according to the manufacturer's instruction,

in HeLa cells. Briefly, the cells were seeded in 96-well tissue culture plate at a density of 5000 cells/well and maintained overnight at 37 °C with 0.1 mL of feeding medium (90% Dulbecco's and 10% fetal calf serum containing 1% antibiotic-antimycotic). After the incubation, the wells were treated with NPs of concentration ranging from 200 µg/ml - 6.25 µg/ml. The cells were then incubated for 24 and 48 hours. The MTT reagent was added to all the wells after each incubation period and then kept for 4 hours at 37 °C. 100 µl of the detergent reagent was finally added and the cells were kept at RT overnight. After the incubation was over, the absorbance in each well was read at 570 nm using a microplate reader (Molecular Devices SpectraMax Plus 384). The controls were cell culture medium, BSA and dodecanedioic acid.

Cell cytotoxicity study using flow cytometry

Cells were seeded in 12-well plates at a density of 2-2.5 × 104 cells per cm^2 and cultured for 24 hours at 37 °C. The cells were washed with fresh media and incubated with various concentrations of NPs, as mentioned in MTT assay, prepared in the culture media. After the treatment, cells were washed twice with 1× PBS to remove residual NPs both in culture media and on the cell surfaces. The media was saved as it contained dead and mitotic cells. The cells were detached using trysin-EDTA and the cells were harvested by centrifugation at 500g for 5 min. The harvested cells were resuspended in PI in appropriate buffer and incubated at room temperature for 15 minutes in the dark. The cells were analyzed using BD FAC Symphony A5 SE equipped with BD FACS Diva software, at an excitation of 488 nm.

Statistical analysis

The MTT assay data was expressed as mean ± standard deviation and the multigroup comparisons of the means were carried out through a one-way analysis of a variance (ANOVA) test and a $p < 0.05$ was considered as statistically significant. Experiments were independently repeated three times at least in triplicate. Error bars in the graphical data represent standard deviations. Results were statistically analyzed using GraphPad Prism v10 (GraphPad Software, San Diego, CA, USA).

Results

Characterization of FluoDot nanoparticles

The hydrodynamic dimensions of the resulting FluoDot nanoparticles were assessed using dynamic light scattering (DLS), revealing a size ranging from 9 nm to 11 nm. Further characterization of FluoDot's morphology and size was conducted via transmission electron microscopy (TEM), confirming a size of approximately 10 nm with a well-defined size distribution and predominantly spherical shape. Zeta potential measurements indicated a net charge of -20 mV. Storage of the nanoparticles in solution phase at 4 °C maintained the secondary structure, with 73% retention observed after exposure to steam sterilization [35].

Cellular uptake of FITC-labeled FluoDot using Confocal Microscopy

The uptake assay revealed that the HeLa cells were able to take in the FluoDot NPs into the cells. The NPs were internalized in a time dependent manner. After the FITC-labeled NPs were added to the cells (10 µg/ml), the fluorescent images were captured at different intervals to analyze the uptake process. It was observed that the NPs were localized in the surface of the plasma membrane of the cells after 30 mins of incubation (Figure 1). The cell membrane was stained with CellMask™ Deep red Plasma Membrane stain which helps to differentiate the FITC-labeled NPs that are attached to the cell surface with those that are inside the cells. Following an hour of incubation, the NPs were internalized by endocytosis into the cells and were no longer found in the plasma membrane. On further incubation of up to 24 hours, we found that most of the fluorescence appears to be inside the cells suggesting that NPs were aggregated near the nucleus and not dispersed around the cytoplasm showing evidence that the NPs were taken up by the cells.

In vitro cell cytotoxicity study of FluoDot NP using MTT assay

The cell viability after treatment of the cells with different concentrations of the NPs were estimated using a commercially available MTT assay. The percentage of cell viability was calculated using the formula:

$$\%\ Cell\ viability = \frac{Mean\ Optical\ Density\ of\ Samples}{Mean\ Optical\ Density\ of\ Media\ Control} \times 100$$

Where optical density is the measure of absorbance of the samples. The optical densities of the samples after different treatments of the NPs were compared with the cells containing only

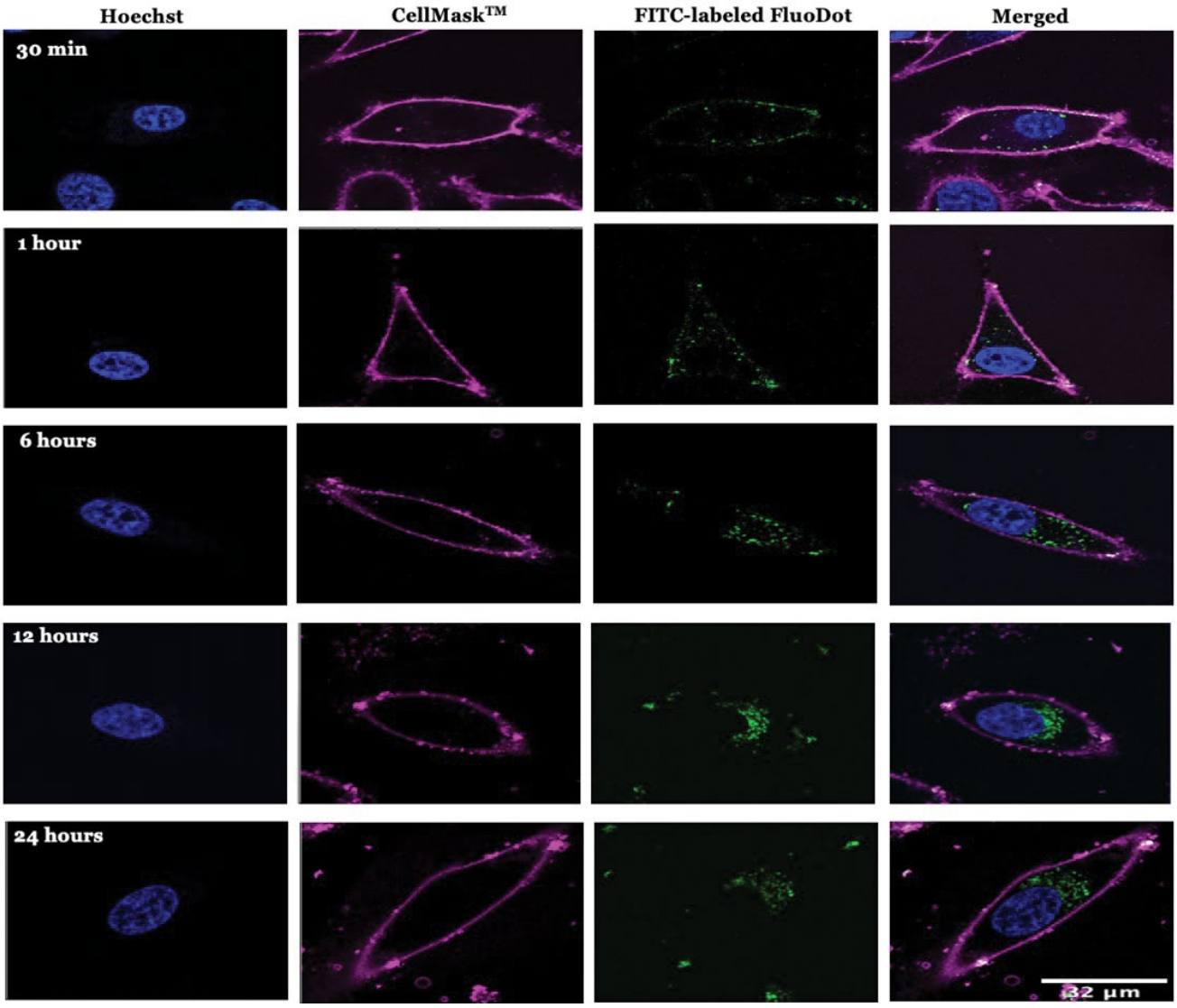

Figure 1: Confocal images of HeLa cells after incubation with FITC-labeled FluoDot NPs (10 µg/ml) at different time intervals (30 min, 1, 6, 12 and 24 hours). The nucleus and cell membrane were stained with Hoechst and CellMaskTN Deep red Plasma Membrane stain, respectively. The internalization of the NP was confirmed by using Nikon A1R Spectral Confocal microscope using × 60 oil immersion lens and analyzed using Image J. *Scale bar*: 32 *µm*.

media, without any treatment, maintained as 100%. The HeLa cells were treated with different concentrations of FluoDot NPs from 200 µg/ml - 6.25 µg/ml at different time intervals (24 hours and 48 hours). Figure 2 shows the cytotoxicity analysis result of the MTT assay. After 24 hours of treatment, the cells showed a significant cell death at a concentration of 25 µg/ml (Figure 2b). Upon further incubation of 48 hours, the significant increase in cell death was seen in the cells treated with concentration of 50 µg/ml of the NP (Figure 2b). As shown in Figure 3a, the cells were also treated with BSA and DDDA, both at a concentration of 200 µg/ml and no cytotoxicity was detected for the two components of the NPs. Based on the cytotoxicity assay, the IC50 of the NP was estimated after 24 hours of incubation. The IC50 concentration was calculated to be 26.4 µg/ml (Figure 3b).

In vitro cell cytotoxicity study of FluoDot NP using flow cytometry

Flow cytometry provides a rapid and more accurate method for measuring viable cells, by differentiating the dead cells from the cell suspension. One of the methods to assess the cell viability is by the use of dye like propidium iodide (PI). PI is a membrane impermeant dye which binds to double stranded DNA by intercalating

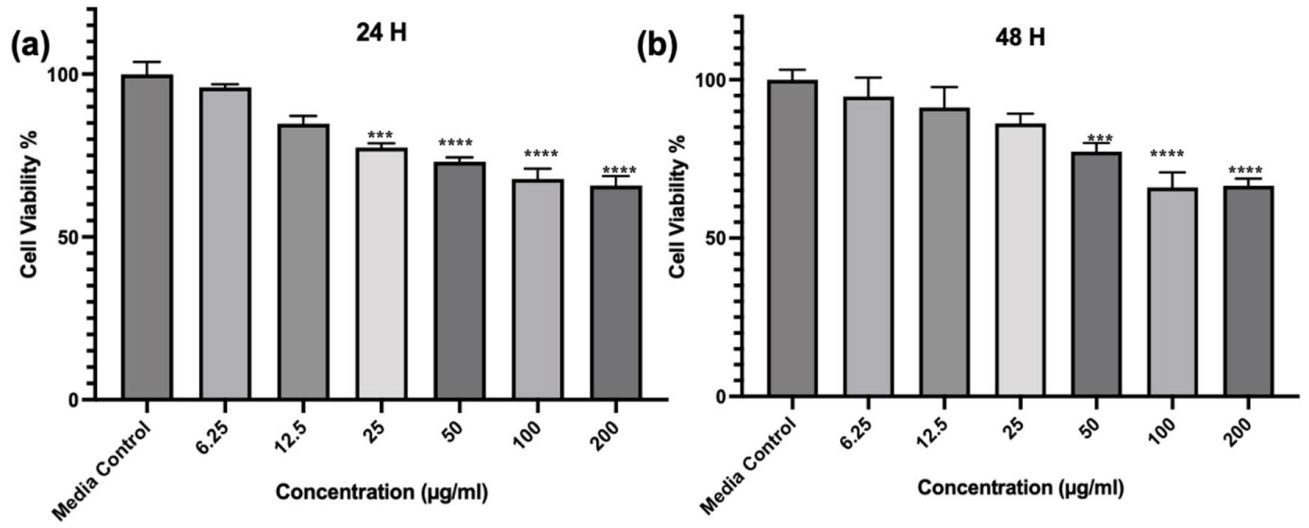

Figure 2: Cell viability of FluoDot NP treated HeLa cells using MTT assay. Cells were treated with 200, 100, 50, 25, 12.5 and 6.25 µg/ml of the NP and incubated at 24 (a) and 48 hours (b). $^{*}P < 0.05$, $^{**}P < 0.01$, $^{***}P < 0.001$ and $^{****}P < 0.0001$.

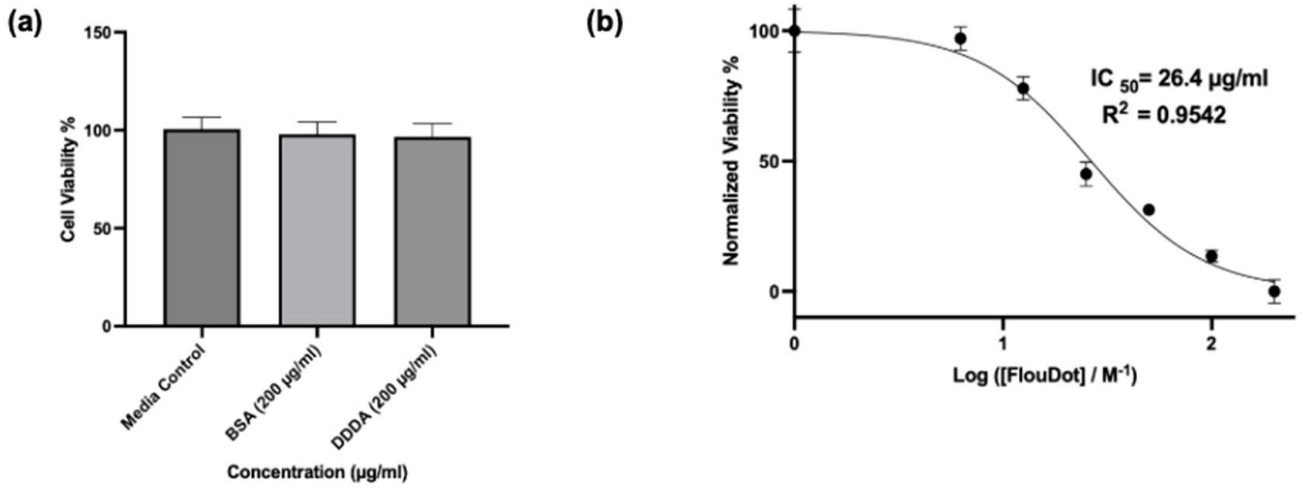

Figure 3: (a) Cell viability assay for media, BSA and DDDA control. (b) IC_{50} cytotoxicity evaluation of FluoDot in HeLa cells using MTT assay. The IC_{50} of the NP was calculated as 26.4 µg/ml using GraphPad Prism v10 software. Data points represent n = 3 experiments with triplicates for each experiment ± standard deviation.

between base pairs. The excitation of PI occurs at 488 nm. A dot plot was established to detect the size (forward scatter [FSC]) and granularity (side scatter [SSC]) using linear scale. The voltage and gain were adjusted with treated and untreated samples in such a way that all the cells (live and dead) were detected based on FSC and SSC and exclusion gates were set to exclude cellular debris. The PI-stained dead cells, which fluoresce brightly, were detectable on the right-hand side of the plot. Each sample were run, and data was acquired for at least 5000 events. The data is represented as dot plot with each dot representing an individual cell. The flow cytometry findings indicate that the cell viability decreases as the concentration of the NP is increased from 3.125 µg/ml to 200 µg/ml indicating the dose-dependent cytotoxicity of FluoDot NP as confirmed by MTT assay (Figure 4).

Discussion

The results of the cellular uptake studies using confocal microscopy revealed time-dependent internalization of the NPs into HeLa, with evidence of agglomeration near the nucleus. The initial localization of NPs on the surface of the plasma membrane after 30 minutes of incubation suggests

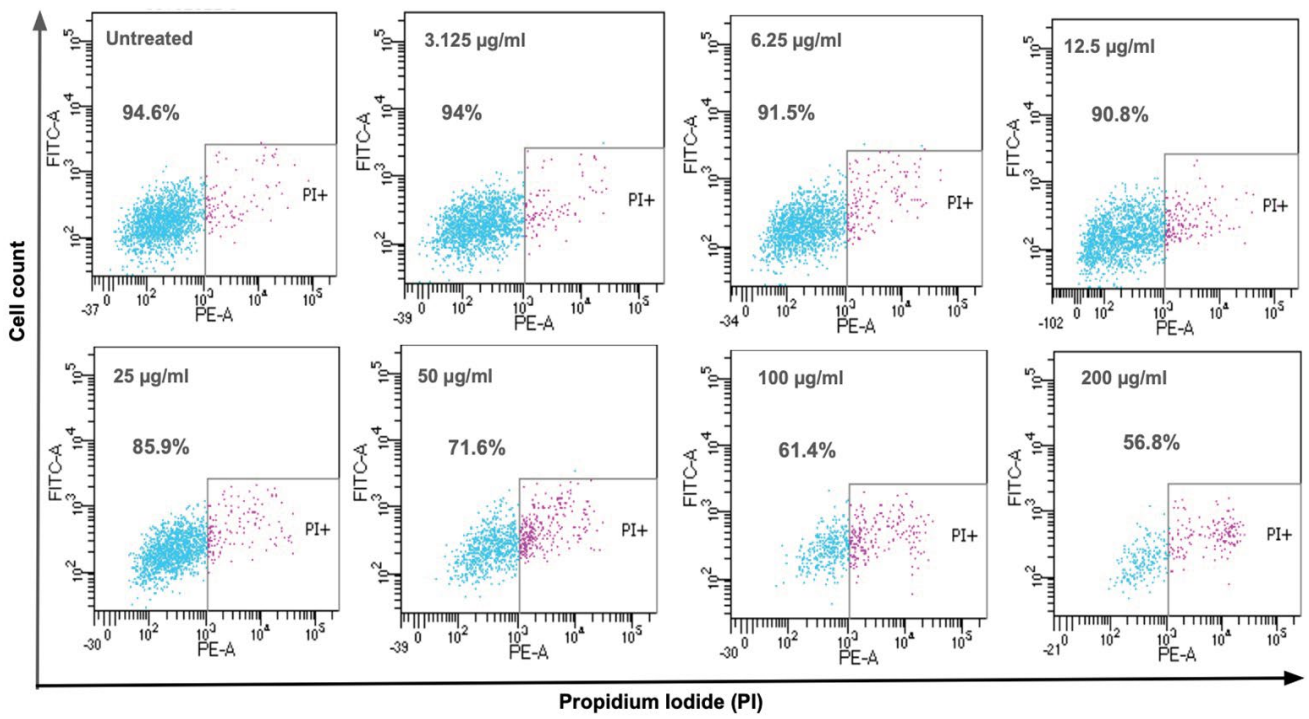

Figure 4: Quantification of cell cytotoxicity to FluoDot NP using Flow cytometry by staining cells using propidium iodide. HeLa cells were treated with different concentrations of FluoDot NPs (200 µg/ml - 3.125 µg/ml) and incubated for 24 hours. Dot plot shows cell count on Y-axis and PI positive cells on X-axis.

an initial interaction between the NPs and the cell membrane. The utilization of CellMask™ Deep Red Plasma Membrane stain facilitated the clarity in tracking the cellular uptake process. The aggregation of NPs near the nucleus, rather than dispersion throughout the cytoplasm, indicates specific cellular targeting or trafficking mechanisms that direct the NPs towards subcellular compartments. This finding supports the hypothesis that the cellular uptake of NPs is not merely a passive process but rather involves active interactions and intracellular transport mechanisms. In addition, the shape of the NP has a tremendous effect on its uptake by cells. Research indicates that the spherical shaped NPs show greater cellular uptake than NPs with other shapes [37-42]. Moreover, the cellular uptake of the NPs is influenced by the surface charge on the NPs. Studies have demonstrated that the anionic NP are internalized by HeLa cells through both clathrin-mediated endocytosis and caveolae-mediated endocytosis [43].

In summary, exposure of the NPs to the HeLa cells showed dose-dependent inhibition of growth of cells which in turn resulted in reduction of viability percentage of the cells. These results indicate that higher the concentration of the NP higher the toxicity to the cells [44]. On exposure to increasing concentrations of NPs, it led to a corresponding decrease in cell viability, with significant cytotoxic effects observed at concentrations of 25 µg/ml after 24 hours and 50 µg/ml after 48 hours of treatment. However, the cell viability percentage at 100 µg/ml is ~70% which is well above the limit of ISO 10993-5: 2009 (Biological evaluation of medical devices part-5: Tests for *in vitro* cytotoxicity) [45] which states that the reduction of cell viability by more than 30% is considered toxic. Furthermore, control experiments with individual components of the NPs, namely BSA and DDDA, did not show any significant cytotoxicity, suggesting that the observed effects are specific to the NPs themselves. Our findings also highlight the importance of factors such as size, shape, surface charge, composition of the NPs and also on the cell type used in mediating the cytotoxicity. While the exact mechanisms underlying NP-induced cytotoxicity remain to be fully elucidated, our results suggest that smaller-sized NPs may exhibit higher toxicity, possibly due to enhanced cellular uptake or interactions with intracellular components. This hypothesis is supported by previous research indicating a correlation between NP size and cytotoxicity [46-53]. Additionally, the determination of the

IC50 concentration, estimated to be 26.4 µg/ml after 24 hours of incubation, provides valuable information for future studies aimed at optimizing NP formulations and assessing their safety profiles.

Finally, our flow cytometry results revealed a clear dose-dependent decrease in cell viability with increasing concentrations of NPs, corroborating findings from the MTT assay. It is noteworthy that the observed differences between flow cytometry and MTT assay data highlight the complementary nature of these techniques; while MTT assay provides an overall assessment of cell viability, flow cytometry offers additional insights by distinguishing between quiescent and actively dividing cells. By combining flow cytometry with other analytical techniques, such as MTT assay, we can gain a deeper understanding of the biological effects of nanoparticles and make informed decisions regarding their suitability for biomedical applications.

Overall, our findings contribute to the growing body of knowledge surrounding the use of nanomaterials in biomedicine, offering new avenues for research and development in the quest for innovative solutions to pressing healthcare challenges. With continued advancements in nanotechnology and biomedicine, FluoDot NPs hold tremendous potential for revolutionizing diagnosis, treatment, and monitoring of diseases, ultimately improving patient outcomes and quality of life.

Author Contributions

Conceptualization: C.K and M.K; Methodology: A.S, J.D, A.K and C.L; Validation: A.S; Investigation: A.S, M.K and C.K; Resources: C.K and M.K; Data curation: A.S; Writing- original draft preparation: A.S; Writing-review and editing: C.K and M.K; Visualization: C.K, M.K and A.S; supervision, C.K and M.K; Project administration: C.K and M.K; Funding acquisition: C.K and M.K. All authors have read and agreed to the published version of the manuscript.

Funding

The authors would like to acknowledge the generous support provided by the National Institute of Food and Agriculture - United States Department of Agriculture (NIFA-USDA) This research was also supported by the Poultry Respiratory Disease Coordinated Agricultural Project (PRD-CAP).

Data Availability Statement

Data available on request from the authors.

Conflicts of Interest

The authors declare no conflicts of interest.

References

1. Couvreur P, Puisieux F (1993) Nano- and microparticles for the delivery of polypeptides and proteins. Adv Drug Deliv Rev 10: 141-162.
2. Couvreur P, Vauthier C (1991) Polyalkylcyanoacrylate nanoparticles as drug carrier: Present state and perspectives. J Controlled Release 17: 187-198.
3. Thurn KT, Brown E, Wu A, Vogt S, Lai B, et al. (2007) Nanoparticles for applications in cellular imaging. Nanoscale Res Lett 2: 430-441.
4. Palazzolo S, Bayda S, Hadla M, Caligiuri I, Corona G, et al. (2018) The clinical translation of organic nanomaterials for cancer therapy: A focus on polymeric nanoparticles, micelles, liposomes and exosomes. Curr Med Chem 25: 4224-4268.
5. Yang H, Qu L, Lin Y, Jiang X, Sun Y-P (2007) Detection of listeria monocytogenes in biofilms using immunonanoparticles. J of Biomed Nanotechnol 3: 131-138.
6. Ai K, Zhang B, Lu L (2009) Europium-based fluorescence nanoparticle sensor for rapid and ultrasensitive detection of an anthrax biomarker. Angewandte Chemie 121: 310-314.
7. Mohanraj VJ, Chen Y (2007) Nanoparticles-A review. Trop J Pharm Res 5: 561-573.
8. Verma D, Gulati N, Kaul S, Mukherjee S, Nagaich U (2018) Protein based nanostructures for drug delivery. J Pharm 2018: 9285854.
9. Lin X, Xie J, Zhu L, Lee S, Niu G, et al. (2011) Hybrid ferritin nanoparticles as activatable probes for tumor imaging. Angew Chem Int Ed 50: 1569-1572.
10. Stromer BS, Roy S, Limbacher MR, Narzary B, Bordoloi M, et al. (2018) Multicolored protein nanoparticles: Synthesis, characterization, and cell uptake. Bioconjugate Chem 29: 2576-2585.
11. Hawkins MJ, Soon-Shiong P, Desai N (2008) Protein nanoparticles as drug carriers in clinical medicine. Adv Drug Deliv Rev 60: 876-885.
12. Jahanshahi M, Babaei Z (2008) Protein nanoparticle: A unique system as drug delivery vehicles. Afr J Biotech 7: 4926-4934.
13. Ping Y, Ding D, Ramos RANS, Mohanram H,

Deepankumar K, et al. (2017) Supramolecular β-sheets stabilized protein nanocarriers for drug delivery and gene transfection. ACS Nano 11: 4528-4541.

14. Stromer BS, Kumar CV (2017) White-emitting protein nanoparticles for cell-entry and pH sensing. Adv Funct Mater 27: 1603874.

15. Sun Q, Chen Q, Blackstock D, Chen W (2015) Post-translational modification of bionanoparticles as a modular platform for biosensor assembly. ACS Nano 9: 8554-8561.

16. Curry S, Mandelkow H, Brick P, Franks N (1998) Crystal structure of human serum albumin complexed with fatty acid reveals an asymmetric distribution of binding sites. Nat Struct Biol 5: 827-835.

17. Baumbach WR, Horner DL, Logan JS (1989) The growth hormone-binding protein in rat serum is an alternatively spliced form of the rat growth hormone receptor. Genes Dev 3: 1199-1205.

18. Bal W, Christodoulou J, Sadler PJ, Tucker A (1998) Multi-metal binding site of serum albumin. J Inorg Biochem 70: 33-39.

19. Elzoghby AO, Samy WM, Elgindy NA (2012) Albumin-based nanoparticles as potential controlled release drug delivery systems. J Control Release 157: 168-182.

20. Sakhrie A, Ding J, Kalluri A, Helal Z, Kumar CV, et al. (2020) Fluodot nanoparticle - a promising novel delivery system for veterinary vaccine. Int J Nanoparticle Res 14.

21. Zhu J, Li J-J, Zhao J-W (2009) Spectral characters of Rhodamine B as a multi-information fluorescence probe for bovine serum albumins. Sens Actuators B: Chem 138: 9-13.

22. Dongmei Z, Xiuhua Z, Yuangang Z, Jialei L, Yu Z (2010) Preparation, characterization, and *in vitro* targeted delivery of folate-decorated paclitaxel-loaded bovine serum albumin nanoparticles. Int J Nanomed 5: 669-677.

23. Chen J, Yu Z, Chen H, Gao J, Liang W (2011) Transfection efficiency and intracellular fate of polycation liposomes combined with protamine. Biomaterials 32: 1412-1418.

24. Clift MJD, Brandenberger C, Rothen-Rutishauser B, Brown DM, Stone V (2011) The uptake and intracellular fate of a series of different surface coated quantum dots in vitro. Toxicology 286: 58-68.

25. Panariti A, Miserocchi G, Rivolta I (2012) The effect of nanoparticle uptake on cellular behavior: Disrupting or enabling functions? Nanotechnol Sci Appl 5: 87-100.

26. Mosmann T (1983) Rapid colorimetric assay for cellular growth and survival: Application to proliferation and cytotoxicity assays. J Immunol Methods 65: 55-63.

27. Maehara Y, Anai H, Tamada R, Sugimachi K (1987) The ATP assay is more sensitive than the succinate dehydrogenase inhibition test for predicting cell viability. Eur J Cancer and Clinical Oncol 23: 273-276.

28. Slater TF, Sawyer B, Sträuli U (1963) Studies on succinate-tetrazolium reductase systems. III. points of coupling of four different tetrazolium salts. Biochim Biophys Acta 77: 383-393.

29. Vistica DT, Skehan P, Scudiero D, Monks A, Pittman A, et al. (1991) Tetrazolium-based Assays for Cellular Viability: A critical examination of selected parameters affecting formazan production. Cancer Research 51: 2515-2520.

30. Darzynkiewicz Z, Bruno S, Del Bino G, Gorczyca W, Hotz MA, et al. (1992) Features of apoptotic cells measured by flow cytometry. Cytometry 13: 795-808.

31. Dangl JL, Parks DR, Oi VT, Herzenberg LA (1982) Rapid isolation of cloned isotype switch variants using fluorescence activated cell sorting. Cytometry 2: 395-401.

32. Krishan A (1975) Rapid flow cytofluorometric analysis of mammalian cell cycle by propidium iodide staining. The J Cell Biol 66: 188-193.

33. Loken MR, Stall AM (1982) Flow cytometry as an analytical and preparative tool in immunology. J Immunol Methods 50: R85-R112.

34. Sasaki DT, Dumas SE, Engleman EG (1987) Discrimination of viable and non-viable cells using propidium iodide in two color immunofluorescences. Cytometry 8: 413-420.

35. Ding J (2019) Multifunctional protein-lipid nanoparticles and hydrogels for biological and environmental applications. Doctoral Dissertations. 2234.

36. Da Silva NIO, Salvador EA, Rodrigues Franco I, De Souza GAP, De Souza Morais SM, et al. (2018) Bovine serum albumin nanoparticles induce histopathological changes and inflammatory cell recruitment in the skin of treated mice. Biomed Pharmacother 107: 1311-1317.

37. Champion JA, Mitragotri S (2009) Shape induced inhibition of phagocytosis of polymer particles. Pharm Res 26: 244-249.

38. Chithrani BD, Ghazani AA, Chan WCW (2006)

Determining the size and shape dependence of gold nanoparticle uptake into mammalian cells. Nano Letters 6: 662-668.

39. Chithrani BD, Chan WCW (2007) Elucidating the mechanism of cellular uptake and removal of protein-coated gold nanoparticles of different sizes and shapes. Nano Letters 7: 1542-1550.

40. Li Y, Kröger M, Liu WK (2015) Shape effect in cellular uptake of PEGylated nanoparticles: Comparison between sphere, rod, cube and disk. Nanoscale 7: 16631-16646.

41. Nel AE, Mädler L, Velegol D, Xia T, Hoek EMV, et al. (2009) Understanding biophysicochemical interactions at the nano–bio interface. Nat Materials 8: 543-557.

42. Zhang B, Sai Lung P, Zhao S, Chu Z, Chrzanowski W, et al. (2017) Shape dependent cytotoxicity of PLGA-PEG nanoparticles on human cells. Sci Rep 7: 7315.

43. Harush-Frenkel O, Debotton N, Benita S, Altschuler Y (2007) Targeting of nanoparticles to the clathrin-mediated endocytic pathway. Biochem Biophys Res Commun 353: 26-32.

44. Lin W, Huang Y, Zhou X-D, Ma Y (2006) In vitro toxicity of silica nanoparticles in human lung cancer cells. Toxicol Appl Pharmacol 217: 252-259.

45. https://www.iso.org/obp/ui/#iso:std:iso:10993:-5:ed-3:v1:en

46. Brown DM, Wilson MR, MacNee W, Stone V, Donaldson K (2001) Size-dependent proinflammatory effects of ultrafine polystyrene particles: A role for surface area and oxidative stress in the enhanced activity of ultrafines. Toxicol Appl Pharmacol 175: 191-199.

47. Karlsson HL, Gustafsson J, Cronholm P, Möller L (2009) Size-dependent toxicity of metal oxide particles-A comparison between nano- and micrometer size. Toxicol Lett 188: 112-118.

48. Li Y, Sun L, Jin M, Du Z, Liu X, et al. (2011) Size-dependent cytotoxicity of amorphous silica nanoparticles in human hepatoma HepG2 cells. Toxicol In Vitro 25: 1343-1352.

49. Midander K, Cronholm P, Karlsson HL, Elihn K, Möller L, et al. (2009) Surface characteristics, copper release, and toxicity of nano- and micrometer-sized copper and copper (ii) oxide particles: A cross-disciplinary study. Small 5: 389-399.

50. Napierska D, Thomassen LCJ, Rabolli V, Lison D, Gonzalez L, et al. (2009) Size-dependent cytotoxicity of monodisperse silica nanoparticles in human endothelial cells. Small 5: 846-853.

51. Wang B, Feng W-Y, Wang T-C, Jia G, Wang M, et al. (2006) Acute toxicity of nano- and micro-scale zinc powder in healthy adult mice. Toxicol Lett 161: 115-123.

52. Warheit DB, Sayes CM, Reed KL (2009) Nanoscale and fine zinc oxide particles: Can in vitro assays accurately forecast lung hazards following inhalation exposures? Environ Sci Technol 43: 7939-7945.

53. Yamamoto A, Honma R, Sumita M, Hanawa T (2006) Cytotoxicity evaluation of ceramic particles of different sizes and shapes. J Biomed Mater Res Part A 68: 244-256.

DOI: 10.35840/2631-5068/5544

Citation: Sakhrie A, Ding J, Kalluri A, Liu C, Kumar CV, et al., (2024) *In-Vitro* Cytotoxicity Assessment and Cellular Uptake Study of Novel FluoDot Nanoparticles on Human Cervical Carcinoma Cells. Int J Nanoparticles Nanotech 9:044